Chapter

Fibril Formation by Glucagon in Solution and in Membrane Environments

Akira Naito

Abstract

Glucagon is a 29-amino acid peptide hormone secreted by pancreatic α-cells and interacts with specific receptors located in various organs. Glucagon tends to form gel-like fibril aggregates that are cytotoxic because they activate apoptotic signaling pathways. First, fibril formation by glucagon in acidic solution is discussed in light of morphological and structural changes during elapsed time. Second, we provide kinetic analyses using a two-step autocatalytic reaction mechanism; the first step is a homogeneous nuclear formation process, and the second step is an autocatalytic heterogeneous fibril elongation process. Third, the processes of fibril formation by glucagon in a membrane environment are discussed based on the structural changes in the fibrils. In the presence of bicelles in acidic solution, glucagon interacts with the bicelles and forms fibril intermediates on the bicelle surface and grows into elongated fibrils. Glucagon-dimyristoylphosphatidylcholine (DMPC) bilayers in neutral solution mimic the environment for fibril formation by glucagon under near-physiological condition. Under these conditions, glucagon forms fibril intermediates that grow into elongated fibrils inside the lipid bilayer. Many days after preparing the glucagon-DMPC bilayer sample, the fibrils form networks inside and outside the bilayer. Furthermore, fibril intermediates strongly interact with lipid bilayers to form small particles.

Keywords: glucagon fibril, fibrillation mechanism, two-step autocatalytic reaction, lipid bilayer, solid-state NMR

1. Introduction

Glucagon is a 29-amino acid peptide hormone secreted by pancreatic α-cells and interacts with specific receptors located in various organs, where it activates the glycogenolysis and gluconeogenic pathways, resulting in raised blood glucose levels [1–3]. Glucagon tends to form gel-like fibrillar aggregates in acidic condition [4]. These aggregates are cytotoxic due to the activation of apoptotic signaling pathways [5]. These fibrils are similar to those of other therapeutic peptides and proteins such as human calcitonin (hCT) [6] and insulin [7] and pathologically related fibrils such as prion [8], amylin (type 2 diabetes) [9], β-amyloid (Alzheimer's disease) [10], and polyglutamine [11].

Some non-fibrillar proteins and peptides have been observed by electron microscopy to form amyloid fibrils with similar morphologies [12].

Several characteristics of these fibrils are related to the misfolding of proteins, leading to severe conditions such as fibril deposits in the brains of Alzheimer's disease patients [13] and in the pancreas of patients with type 2 diabetes [9].

Kinetic analyses of fibril formation by the therapeutic peptide human calcitonin indicate that hCT molecules associate to form fibril intermediates via a two-step autocatalytic reaction mechanism. The first step of kinetic reaction (rate constant, k_1) is a homogeneous reaction from micelle-like oligomers to fibril intermediates. These intermediates react with monomeric molecules to elongate into longer fibrils via a heterogeneous fibril elongation process (rate constant, k_2) [14–17]. Elucidating the molecular structure of amyloid fibrils is important for understanding the mechanism of self-aggregation, but it is difficult to determine high-resolution molecular structures using typical spectroscopic methods because fibrils are heterogeneous solids. Solid-state NMR spectroscopy has demonstrated advantages for the conformational determination of Alzheimer's amyloid β-peptides (Aβ), which mainly comprise 40 or 42 amino acid residues and are the main component of the amyloid plaques found in Alzheimer's disease patients [12, 18]. Both the intra-chain conformation of the Aβ molecule in fibrils and their intermolecular alignment have been analyzed to explore the mechanism of molecular association underlying the formation of Aβ (1–40) [19–21] and the more toxic Aβ (1–42) [22–24] fibrils.

The primary structure of the glucagon peptide is His^{1}-Ser-Gln-Gly-Thr^{5}-Phe-Thr-Ser-Asp-Tyr^{10}-Ser-Lys-Tyr-Leu-Asp^{15}-Ser-Arg-Arg-Ala-Gln^{20}-Asp-Phe-Val-Gln-Trp^{25}-Leu-Met-Asn-Thr-OH.

An X-ray crystallographic study showed that glucagon adopts a trimeric α-helix structure stabilized by hydrophobic interactions between molecules related by threefold symmetry [25], whereas a solution NMR study showed that glucagon in dilute aqueous solution may not form a specific structure, with the exception of the 22–25 region [26]. The secondary structure of glucagon in the presence of dodecylphosphocholine micelles comprises three turns of an irregular α-helix formed by residues 17 to 29 near the C-terminus, a stretch of extended polypeptide chain from residues 14 to 17, an α-helix-like turn formed by residue 10 to 14, and another extended region from residue 5 to 10 [27].

Fibril formation by glucagon molecules was observed by Beaven et al. in undisturbed aqueous solution at pH 2 [4]. The viscosity initially increased and a birefringent gel is formed. With time, a precipitate appeared comprising long fibrils, as determined using electron microscopy. Infrared spectra of the gel, solid film, and precipitate showed that in all these states, glucagon is in the form of antiparallel β-sheet chains [5, 28]. Kinetic analysis of fibril formation by glucagon under acidic conditions demonstrated a complex fibrillation mechanism in which suitable changes in the fibrillation condition can alter the type of fibril formed or result in the formation of a mixture of several types of fibrils [29, 30]. Furthermore, the fibrils come in two forms: one composed entirely of glucagon monomers and the other entirely of glucagon trimers [31]. Studies of fibril formation typically use acidic pH solutions because of the low solubility of glucagon in neutral solution.

Understanding the cytotoxicity of amyloid-forming peptides requires investigating the interaction of these peptides with membranes because lipid bilayer components dramatically alter most aspects of amyloid aggregation [32–35]. We previously reported glucagon fibrillation in the presence of dimyristoylphosphatidylcholine/1,2-dihexanoyl-sn-glycero-3-phophocholine (DMPC-DHPC) bicelles in acidic solution. The glucagon structure in the fibril in the presence of these bicelles is different from that in their absence [36]: the N- and C-termini both change from α-helix to β-sheet in acidic solution, while the N-terminus remains in an α-helical conformation, whereas the C-terminus changes from α-helix to β-sheet in the

presence of bicelles. The nucleation rate is slower, and the fibril elongation rate is faster in acidic solution than in the presence of bicelles.

In neutral conditions, glucagon molecules are incorporated into lipid bilayers above the phase transition temperature, and the properties of the lipids appear to remain unperturbed. Below the phase transition temperature, glucagon forms discoidal particle with DMPC [37, 38] and induces closer packing of the phospholipid bilayers [39]. Similar peptide-lipid interaction to form discoidal particles below the phase transition temperature is seen in the melittin-DMPC bilayer system [40, 41].

The time course behavior of glucagon fibril formation inside a DMPC bilayer under neutral conditions, which approximates the physiological condition, and the kinetic behavior of glucagon under these conditions have been investigated to understand the fibrillation process under near-physiological conditions [42].

2. Fibril formation by glucagon in acidic solution

Gel formation by glucagon in the β-sheet conformation in acid solutions is a relatively slow process at room temperature [4] and can be followed by observing the change in viscosity as shown in **Figure 1**. The most marked feature of the change in viscosity in these time profiles is the presence of a substantial lag phase during which oligomeric nuclei are likely formed and function as initiation sites. These phenomena were confirmed by adding a small seed of preformed glucagon gel on the end of a wire into a viscometer containing a fresh acidic glucagon solution. The viscosity increased immediately with essentially no lag (**Figure 1a**). After a prolonged reaction time, the viscosity began to decrease and fibrils sometimes precipitated. These fibrils represent a variant of the β-structure of glucagon.

Fibril formation strongly depends on the peptide concentration, proceeding very slowly at less than about 1.5 mg/ml and occurring more readily at higher concentration (**Figure 1b**). Increasing the ionic strength of the solution results in both an increasing aggregation rate and more rapid production of fibrils. The change in viscosity with time in even 0.01 M sodium chloride occurs much more rapidly than in the absence of salt, and viscosity decreases quickly.

The effect of temperature on the polymerization rate is also very marked. Both the aggregation rate and the size of the aggregates as reflected in the maximal values of the reduced viscosity show a strong temperature maximum around 30°C (**Figure 1c**). An addition of 5% (v/v) of the nonaqueous solvent dioxin completely inhibits the aggregation (**Figure 1a**).

Transmission electron microscopy (TEM) time-elapsed pictures were obtained during fibril formation by glucagon dissolved in 0.015 M acetic acid solution (18 mg/ml) at pH 3.3 [36]. TEM pictures were measured approximately 2 hrs, then 1 week, and 6 months after the dissolution of glucagon (**Figure 2**). A small number of spherical-shaped fibril intermediates appeared after approximately 2 hrs, as shown in **Figure 2a**. After 1 week, the number of spherical fibril intermediates had increased, and elongated fibrils had appeared (**Figure 2b**). After 6 months, long mature fibrils about 10 nm in diameter were observed, and the spherical fibril intermediates had completely disappeared (**Figure 2c**).

The α-helical content of aged glucagon at 5.0 mg/ml decreased significantly to approximately 1%. The CD spectrum of a β-sheet structure typically shows an intense positive band at 198 nm and a negative band at 218 nm [5]. The CD spectral pattern of aged glucagon was that of a β-sheet structure, indicating a conformational transition from α-helical to β-sheet structure under these conditions.

The FTIR spectrum of glucagon immediately after dissolution showed a low-intensity β-sheet band at 1620–1630 cm^{-1}, and aging resulted in progressively

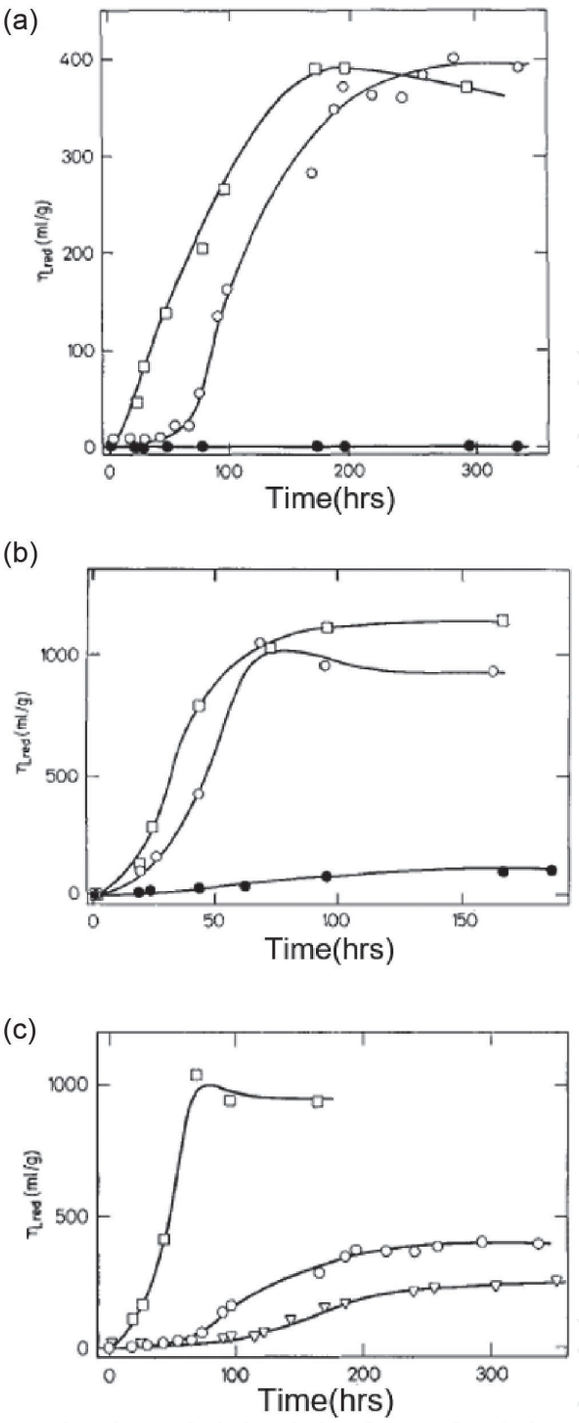

Figure 1.
Time course behavior of glucagon aggregation in 0.01 M hydrochloric acid at 26°C and a glucagon concentration of 2.5 mg/ml. (a) Time course of reduced viscosity (msp/c); glucagon with no addition (○); glucagon seeded with preformed gel (□); glucagon solution containing 5% by volume dioxin (●). (b) Effect of glucagon concentration at 4 mg/ml (□); 2.5 mg/ml (○); and 1 mg/ml (●). (c) Effect of temperature on the aggregation rate of glucagon at a glucagon concentration of 2.5 mg/ml at 26°C (○); 30°C (□); and 35°C (▽) (ref. [4]).

greater amounts of β-sheet [28]. Deconvolution and curve fitting of the amide I band showed that unaged glucagon contained 54% α-helix/random coil structure and 2% β-sheet structure, whereas aged glucagon comprised 22% α-helix/random coil structure and 49% β-sheet structure.

Detailed kinetic, spectroscopic, and morphological studies have revealed that glucagon can form several types of fibrils that differ at the level of molecular packing of the peptide [29–31, 43–46]. Each type forms through distinct

nucleation-dependent aggregation pathways influenced by the solution conditions and can be self-propagated by seeding. Type A fibrils that form at high glucagon concentration (>5 mg/ml, pH 2.5) represent the least stable fibril type with a low melting midpoint (T_{mapp} < 32°C) and single protofilament fibrils observable by TEM (**Figure 3a**). Type B ($B_{unagitated}$ and $B_{agitated}$) fibrils form under low glucagon concentration (<0.5 mg/ml, pH 2.5). Type $B_{unagitated}$ fibrils grow by branching in the absence of agitation and appear as branched twisted fibrils by TEM (**Figure 3b**). Type $B_{agitated}$ glucagon fibrils form when the solution is agitated, suggesting that agitation breaks the fibril creating more free fibril ends that align as parallel pairs (**Figure 3c**). Type D fibrils grow under low glucagon concentration (<0.5 mg/ml, pH 2.5) in the presence of 150–250 mM Cl^- and are twisted and tightly packed

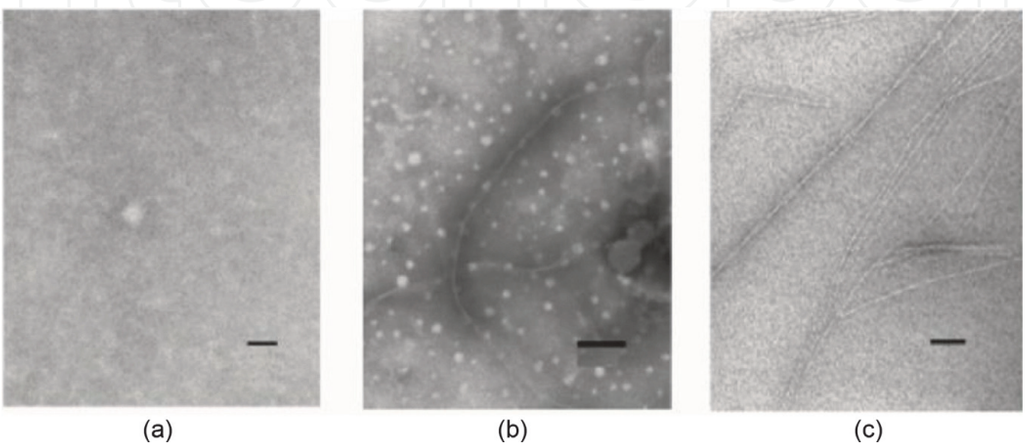

Figure 2.
Transmission electron micrographs of glucagon (18 mg/ml) in 0.015 M acetic acid solution at pH 3.3. (a) Taken approximately 2 hrs after the dissolution of glucagon. The bar indicates 20 nm. (b) Taken 1 week after dissolution of glucagon. The bar indicates 50 nm. (c) Taken 6 months after dissolution of glucagon. The bar indicates 50 nm (ref. [36]).

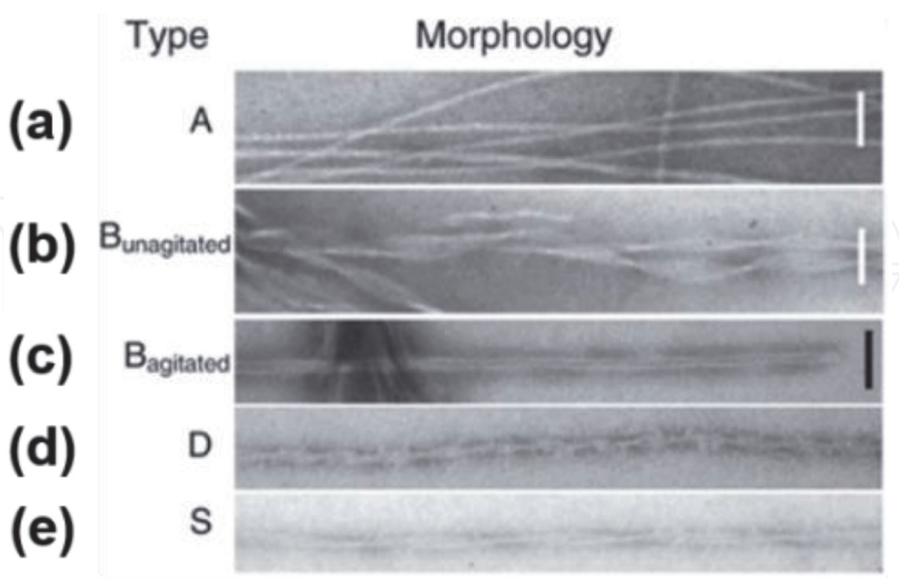

Figure 3.
Electron microscope image of morphology of different types of glucagon fibrils. The scale bar is 50 nm. (a) Type A: The glucagon concentration, >5 mg/ml, 50 mM glycine, pH 2.5, low agitation. (b) Type $B_{unagitated}$: Glucagon concentration, <0.5 mg/ml, 50 mM glycine, pH 2.5, low agitation. (c) Type $B_{agitated}$: Glucagon concentration, <0.5 mg/ml, 50 mM glycine, vigorous agitation. (d) Type D: Glucagon concentration, <0.5 mg/ml, 50 mM glycine, pH 2.5+, 150–250 mM Cl^-. (e) Type S: Glucagon concentration, <0.5 mg/ml, 0.01 N HCl, 1 mM SO_4^{2-} (ref. [30]).

(**Figure 3d**). Type S fibrils grow under low glucagon concentration (<0.5 mg/ml, pH 2.5) in the presence of 1 mM Na_2SO_4 (7:1 ratio with glucagon) and appear as twisted mature fibrils by TEM (**Figure 3e**).

Solid-state ^{13}C NMR spectra were observed for 18 mg/ml [1-^{13}C]Gly4 and [3-^{13}C]Ala19-glucagon in 0.015 M acetic acid solution, pH 3.3 [36]. The ^{13}C direct excitation with dipolar decoupling and magic angle spinning (DD-MAS) signal indicates monomeric glucagon, and the ^{13}C cross polarization with magic angle spinning (CP-MAS) signal indicates fibril glucagon. The DD-MAS spectra (**Figure 4A** and **C**) of [1-^{13}C]Gly4 and [3-^{13}C]Ala19 exhibit signals at 171.7 and 16.4 ppm, respectively, consistent with the monomeric state and indicate that the region near the Gly4 and Ala19 residues forms α-helix structures, as shown by the conformationally dependent chemical shift values [47–49]. The experimentally determined chemical shift values and secondary structures are summarized in **Table 1**. The ^{13}C CP-MAS spectra of [1-^{13}C]Gly4 and [3-^{13}C]Ala19 (**Figure 4B** and **D**)

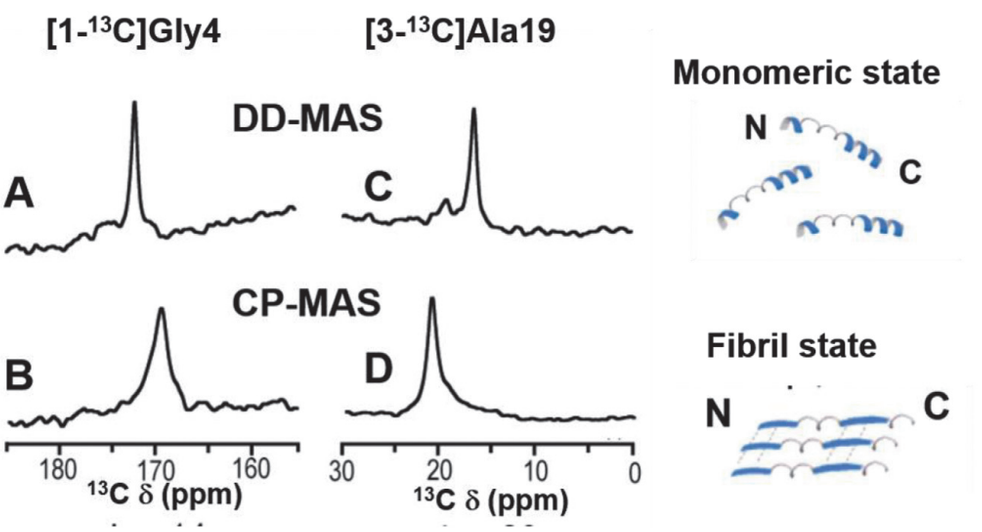

Figure 4.
^{13}C DD-MAS and CP-MAS NMR spectra of [1-^{13}C]Gly4 (A and B) and [3-^{13}C]Ala19 (C and D) of [1-^{13}C]Gly4 and [3-^{13}C]Ala19-glucagon in acetic acid solution at pH 3.3. Schematic structures of glucagon in the monomeric and fibril states (right panels) (ref. [36]).

Fibril formation condition	Fibril type	[1-^{13}C]Gly4 (structure)	[3-^{13}C]Ala19 (structure)	Ref.
Acidic solution (0.015 M acetic acid solution pH 3.3)	Monomer	171.7 (α-helix)	16.4 (α-helix)	[36]
	Fibril	169.2 (β-sheet)	21.0 (β-sheet)	[36]
Acidic solution in the presence of bicelle (DMPC+DHPC pH 3.3)	Monomer	171.5 (α-helix)	16.4 (α-sheet)	[36]
	Fibril	171.5 (α-helix)	19.3 (β-sheet)	[36]
Glucagon inside lipid bilayer (DMPC) in neutral solution	Monomer	171.5 (α-helix)	15.9 (α-helix)	[42]
	Intermediate	168.9 (β-sheet)	20.5 (β-sheet)	[42]
	Fibril	166.9 (β-sheet)	21.5 (β-sheet)	[42]

**The structure around each amino acid residues was determined by comparing the experimentally obtained ^{13}C chemical shift values (δ_{iso}) with typical ^{13}C chemical shift values (δ_{iso}) of α-helix and β-sheet, reported as 171.6 and 168.5 for [1-^{13}C]Gly and 14.9 and 19.9 for [3-^{13}C]Ala, respectively [47–49].*

Table 1.
Structural transitions during glucagon fibrillation in various conditions as determined by conformation-dependent ^{13}C chemical shifts (ppm).*

of glucagon in the fibril state exhibit signals at 167.2 and 21.0 ppm, respectively, and indicate that the vicinities of Gly4 and Ala19 form β-sheet structures.

Conformationally dependent chemical shift values [47–49] clearly indicate that the N-terminus of monomeric glucagon forms an α-helix structure, the center portion forms a random coil, and the C-terminus forms an α-helix structure, as shown in **Table 1** and **Figure 4** (right panels) in acetic acid solution. When the glucagon monomer aggregates to form fibrils, the N-terminal and C-terminal regions change from an α-helix to a β-sheet as seen with other amyloid-forming peptides such as human calcitonin [14] in acetic acid solution.

3. Cytotoxicity of glucagon fibril

The cytotoxicity of the glucagon fibril was assessed by exposing PC12 and NIH-3 T3 cells to 0.1–100 μM peptide aggregate for 72 hrs followed by cell viability determination under the WST-8 assay and released lactate dehydrogenase (LDH) [5]. A significant decrease in cell viability was observed in cultures exposed to 10–100 μM aged glucagon ($P < 0.01$) but not in cultures treated with 100 μM nonaged glucagon. It was determined whether the loss of cell viability was due to cell death by measuring the release of LDH. Treatment with 10 μM aged glucagon induced a significant increase in LDH release compared to control, whereas no significant increase in LDH release was observed in cultures treated with 100 μM nonaged glucagon or 1 μM or lower aged glucagon. Thus, glucagon fibrils were found to be highly toxic to PC12 cells, similar to the case of aged prion protein fragment (PrP)106–126 [50] and β-amyloid (Aβ)1–42 [51] (>10 mM). Aged salmon calcitonin also displayed significant cytotoxicity in PC12 cells, whereas nonaged salmon calcitonin did not induce significant cell death [5].

Next, signaling pathways for the cytotoxicity of peptide fibrils were investigated [5]. Caspase-3 activation is required for the early stages of apoptosis that include DNA fragmentation and morphological changes. To determine whether aged glucagon induces caspase-3 activation in PC12 cells, cells were exposed to 50 μM aged glucagon, and the caspase-3-like activities of the cell lysates were measured by cleavage of the fluorometric caspase-3 substitute Z-DEVD-rhodamine 110. The activity increased prior to the loss of membrane integrity, and 24 hrs after incubation, maximum caspase-3 activity was detected (160% of the control level). In contrast, no significant elevation of casepase-3 activity was observed in cells treated with 50 μM nonaged glucagon. These results indicate that the exposure of PC12 cells to peptide fibrils induces a rapid (within 24 hrs) and significant elevation in casepase-3 activity prior to the loss of cell viability 72 hrs after exposure.

In summary, the misfolding of the therapeutic peptide glucagon generates amyloidogenic fibrils, leading to cytotoxicity mediated by the activation of the apoptotic enzyme caspase-3 in vitro.

4. Kinetic analysis of the glucagon fibrillation process

As shown in **Figure 5**, glucagon monomers (A) first aggregate to form weakly coupled oligomers (A_n) akin to the micelle state. Next, glucagon oligomers (A_n) form fibril intermediates (nuclei) (B_n) through a homogeneous nucleation process with a rate constant k_1. Fibril intermediates (B_n) then react with monomer (A) to form elongated fibrils with a rate constant k_2. This is called the inhomogeneous fibril elongation process. The B form plays a role in the catalysis of A to B, and therefore this is an autocatalytic reaction. Since the nucleation and elongation

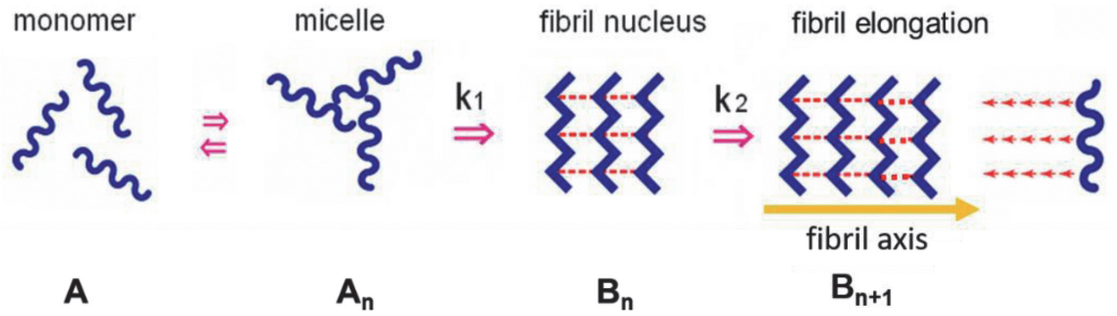

Figure 5.
Schematic of the glucagon fibril formation process in acidic solution. Several monomers (A) aggregate to form weakly coupled micelles (A_n). Micelles (A_n) form a fibril nucleus (B_n) through a homogeneous nucleation process with a rate constant k_1. Fibril nuclei react with monomers (A) to form elongated fibrils (B_{n+1}) with a rate constant k_2. In this reaction, B acts as a catalyst to change the A form to the B form. Overall, this fibril formation reaction is a two-step autocatalytic reaction mechanism.

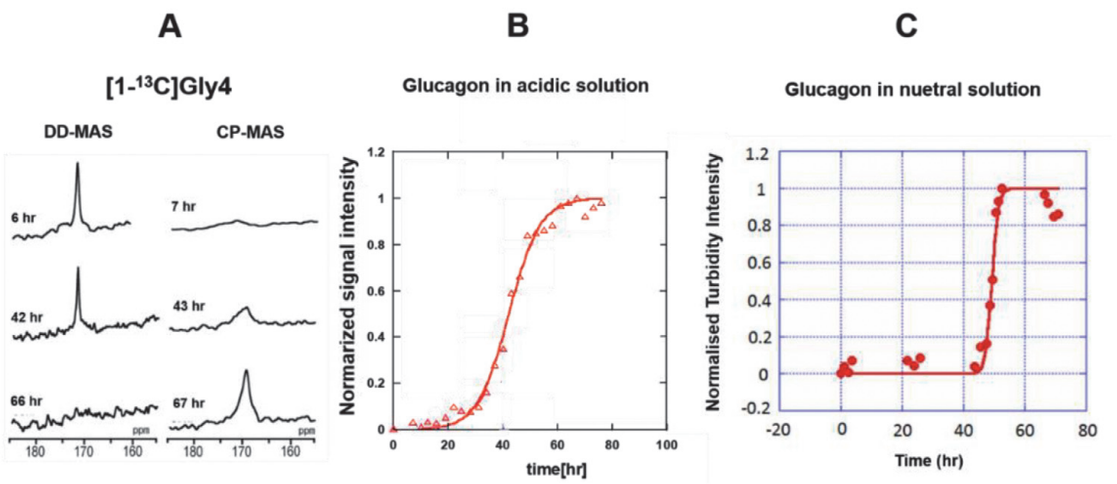

Figure 6.
(A) Time course of changes in the ^{13}C CP-MAS and DD-MAS signals of [1-^{13}C]Gly-glucagon during the fibril formation processes [36]. (B) Plot of normalized CP-MAS signal intensity against elapsed time for glucagon fibril formation in acidic solution at pH 3.3 [36]. (C) Plot of normalized turbidity intensities against elapsed time for glucagon fibril formation in neutral solution (20% acetonitrile solution, pH 7.5) [42].

processes are rate-determining steps, fibril formation is a two-step autocatalytic reaction.

The rate constants of glucagon fibril formation were determined by observing the signal intensities of [1-^{13}C]Gly4 in [1-^{13}C]Gly4 and [3-^{13}C]Ala19-glucagons by ^{13}C CP-MAS NMR spectroscopy with time (**Figure 6A** and **B**). The signal intensities increased after a delay time. The increase in ^{13}C CP-MAS signal intensities corresponds to the increase in fibril components, and thus we obtained the rate constants, k_1 and k_2, for the two-step autocatalytic reaction mechanism, in which k_1 is the rate constant for the fibril nucleation process and k_2 is the rate constant for the fibril elongation process [14].

The first reaction step is homogeneous nuclear formation given by

$$A_{no} \xrightarrow{k_1} B_{no}, \tag{1}$$

where A_{no} is the micelles formed by n_o number of A-form glucagon monomers and B_{no} is the fibrils formed by n_o number of B-form glucagon fibrils. The kinetic equation for Reaction (1) can be given by

$$(df/dt)_1 = k_1(1-f), \tag{2}$$

where *f* is the fraction of B-glucagon fibrils in the system.

The second heterogeneous fibril elongation reaction can be given by k_2

$$A + B_n \xrightarrow{k_2} B_{n+1}, \tag{3}$$

where B_n and B_{n+1} are elongated fibrils with n and n + 1 number of B-form glucagons. The relevant kinetic equation is given by

$$(df/dt)_2 = k_2 a f(1-f), \tag{4}$$

where a is the initial concentration of glucagon. The overall kinetic equation can be given by

$$(df/dt) = (df/dt)_1 + (df/dt)_2 = k_1(1-f) + k_2 a(1-f), \tag{5}$$

Eq. (5) can be integrated to give

$$f = \frac{\rho\{\exp[(1+\rho)kt] - 1\}}{\{1 + \rho\exp[(1+\rho)kt]\}} \tag{6}$$

where *f* is the fraction of glucagon molecules in the fibril form at time *t* and ρ represents a dimensionless value describing the ratio of k_1 (the rate constant for the first nucleation process) to k, namely, $\rho = k_1/k$ and $k = ak_2$ (k_2 is the rate constant for the second elongation process of the fibrils, and a is the initial peptide concentration) [14]. The best fits of Eq. (6) are shown in **Figure 6B** (solid lines), and the analyzed rate constants are summarized in **Table 2**. The k_1 and k_2 values were obtained experimentally from the intensity variation of the ^{13}C CP-MAS NMR signals of [1-^{13}C]Gly4 as shown in **Figure 6B** and **Table 2** for glucagon in acidic solution. In comparison, rate constants of fibril formation were obtained for glucagon in neutral solution by plotting the turbidity of the solution against the elapsed time by using an established protocol [52] (**Figure 6C**).

The intensity of the ^{13}C CP-MAS NMR signal of [1-^{13}C]Gly4 was plotted against the elapsed time for glucagon in the presence of bicelles in acidic solution and for glucagon embedded inside lipid bilayers in neutral solution. The obtained rate constants are given in **Table 2**.

Fibril formation condition	**k_1 (s^{-1})**	**k_2 ($s^{-1}M^{-1}$)**	**Ref.**
Acidic solution (0.015 M acetic acid pH 3.3)	2.6×10^{-8}	1.8×10^{-2}	[36]
Neutral solution (20% acetonitrile pH 7.5)	1.2×10^{-24}	4.4×10	[42]
Acidic solution (pH 3.3) in the presence of bicelle (DMPC+DHPC)	2.3×10^{-6}	2.8×10^{-3}	[36]
Inside a lipid bilayer (DMPC) in neutral solution (pH 7.5)	2.8×10^{-7}	5.7×10^{-4}	[42]

Table 2.
Rate constants for glucagon fibril nucleation (k_1) and fibril elongation (k_2) for a two-step autocatalytic reaction mechanism under a variety of conditions.

5. Fibril formation by glucagon in the presence of bicelles in acidic solution

In the presence of bicelles (DMPC-DHPC; 3:1), the N-terminus of glucagon forms an α-helix, the center portion forms a random coil, and the C-terminus forms

an α-helix in the monomeric state (**Table 1**). In contrast to glucagon in acetic acid solution, the aggregation of monomers into the fibrils in the presence of bicelles results in the N-terminus maintaining an α-helix structure and the center portion remaining in a random coil structure, whereas the C-terminus changes from an α-helix to a β-sheet structure (**Figure 7** and **Table 1**). There is therefore significant difference in the structural transition between monomer and fibril in the presence and absence of bicelles, since the N-terminus maintains an α-helix structure in the process of fibril formation in the presence of bicelles. This result suggests that the N-terminal portion of a glucagon fibril significantly interacts with the lipid bilayer surface.

The above findings provide insights into the mechanism of fibril formation in the presence and absence of lipid bilayers, as shown in **Figure 7**. In the absence of lipid bilayers, monomers may aggregate with each other to form oligomeric intermediates (similar to micelles) through a homogeneous reaction (**Figure 7B**; left), likely driven by the amphipathic natures of the N-terminal and C-terminal α-helices. These oligomeric intermediates then change into spherical fibril intermediates (**Figure 7C**; left) as observed by TEM (**Figure 2a** and **b**). Subsequently, these spherical fibril intermediates may form fibril nuclei and interact with monomeric glucagon to allow elongation of the fibril by changing from an α-helix to a β-sheet through a heterogeneous elongation process (**Figure 7D**; left).

In the presence of lipid bilayers, monomers form a structure similar to that in the absence of lipid bilayers. The monomers likely associate quickly with the lipid bilayer and subsequently associate with other monomers to form weakly coupled oligomeric intermediates (**Figure 7B**; right). These oligomeric intermediates may change their structure to form fibril intermediates on the surface of the lipid bilayer and are observed as ellipsoid-shaped fibril intermediates (**Figure 7C**; right and TEM picture) on the surface of the lipid bilayer. The elliptical shape is due to the N-terminal region retaining an α-helix structure even in the fibril intermediates.

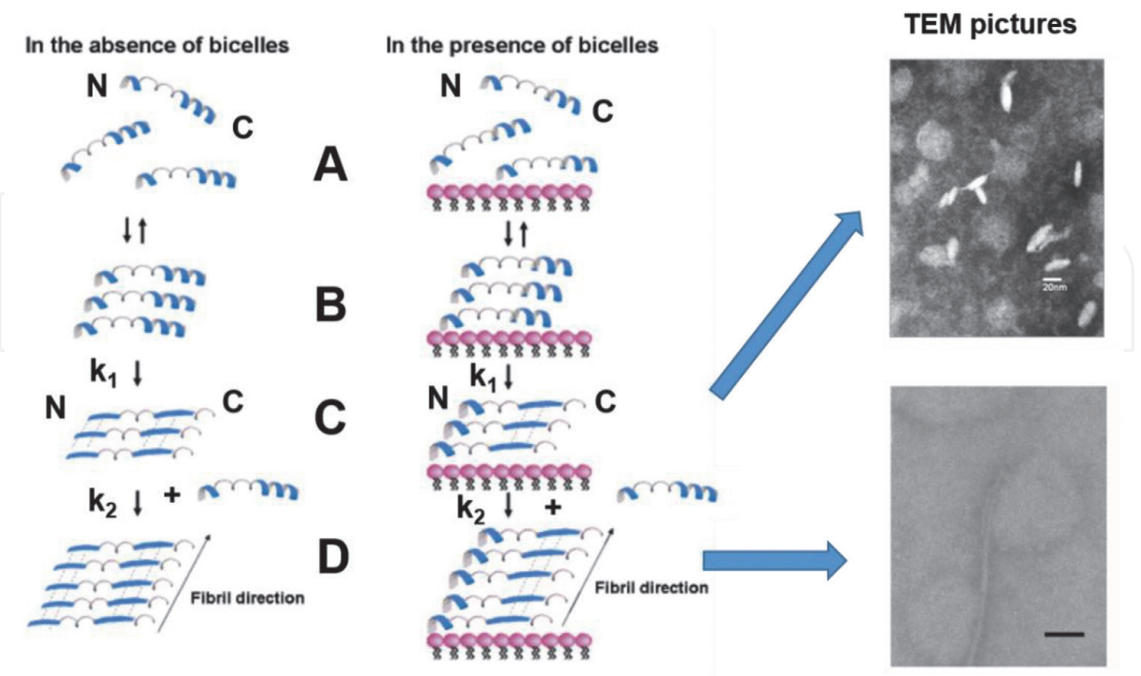

Figure 7.
Schematic diagram of the fibrillation processes of glucagon in acetic acid solution (left) and acidic solution in the presence of bicelles (center). (A) Monomeric form. (B) Weakly coupled oligomer. (C) Fibril intermediate. (D) Elongated fibril. TEM pictures of glucagon fibril intermediates with ellipsoidal shapes and of disk-type bicelles are seen in the top right photo. An elongated fibril is seen attached by its end to a bicelle in the bottom right photo (ref. [36]).

The fibril intermediates grow into longer fibrils on the surface of the lipid bilayer and protrude outside the lipid bilayers, as shown schematically in **Figure 7D** (right) and in the TEM picture (**Figure 7D**; right bottom).

The k_1 rate constant for nuclear formation in the presence of lipid bilayers is faster than in the absence of lipid bilayers (**Table 2**) because glucagon monomers associate with the surface of the lipid bilayer, migrate laterally on the surface of the lipid bilayer to form oligomeric intermediates, and then subsequently change to fibril intermediate through a homogeneous nucleation reaction. This two-dimensional process may be faster than nuclear formation in the three-dimensional solution state.

The k_2 rate constant for fibril elongation in the presence of lipid bilayers is slower than in the absence of lipid bilayers. As discussed previously, the N-terminal part of the glucagon molecule in a fibril in the presence of a lipid bilayer remains in an α-helix which may be stabilized when the helix interacts with the lipid bilayer. However, after the fibril grows and is released from the lipid bilayer, the N-terminal α-helix becomes more unstable than the N-terminal β-sheet formed in a fibril that protrudes from the lipid bilayer. This unstable fibril can grow to the outside of the lipid bilayer because it potentially acts as a template to form structures identical to the fibril nuclei formed on the surface of the lipid bilayer. The instability of the fibril state outside the lipid bilayer results in a decrease in the k_2 value for fibril elongation as compared to the absence of a lipid bilayer.

These results show that glucagon molecules significantly interact with lipid bilayers during the fibril formation processes. To understand the fibril formation process under physiological condition, a variety of lipid bilayer systems including a lipid bilayer in neutral solution were investigated.

6. Fibrillation mechanism of glucagon inside the lipid bilayer in the neutral condition

Fibril formation processes were investigated for glucagon embedded inside a lipid bilayer in neutral solutions (i.e., essentially physiological conditions) [42]. Glucagon-induced morphological changes of lipid bilayers and fibril formation process in a glucagon containing lipid bilayer are shown in **Figure 8**. The monomers may aggregate with each other to form oligomers (**Figure 8B**) likely driven by the amphipathic nature of the N-terminal and C-terminal α-helices. These oligomers then change into ellipsoidal fibril intermediates (nuclei) (**Figure 8C**) through a homogeneous reaction, as observed by TEM (**Figure 8C**, bottom). At this stage, the glucagon intermediates strongly interact with the lipid bilayer to form discoidal lipid bilayer particles. Subsequently, this ellipsoidal fibril intermediate (nucleus) interacts with monomeric glucagon inside the lipid bilayer to allow elongation of the fibril by changing from an α-helix to a β-sheet through a heterogeneous elongation process (**Figure 8D**). After a long time standing, fibril networks are formed, and lipid molecules are compartmentalized (**Figure 8E**), resulting in increased lipid molecule mobility and the induction of a gel-like state throughout the sample, now in an amyloidogenic gel state [53, 54].

The kinetic of fibrillation was thus analyzed using a two-step autocatalytic mechanism as summarized in **Table 2**. The k_1 rate constant for nuclear formation in neutral solution is much slower than that in a DMPC bilayer in neutral conditions (**Table 2**). In a DMPC/glucagon bilayer, glucagon molecules are condensed inside the DMPC bilayer, and thus the nucleation rate of glucagon in a DMPC/glucagon bilayer is much faster than that in neutral solution. The k_1 rate constant for nuclear formation in a lipid bilayer in a neutral solution is slower than in a lipid bilayer in an

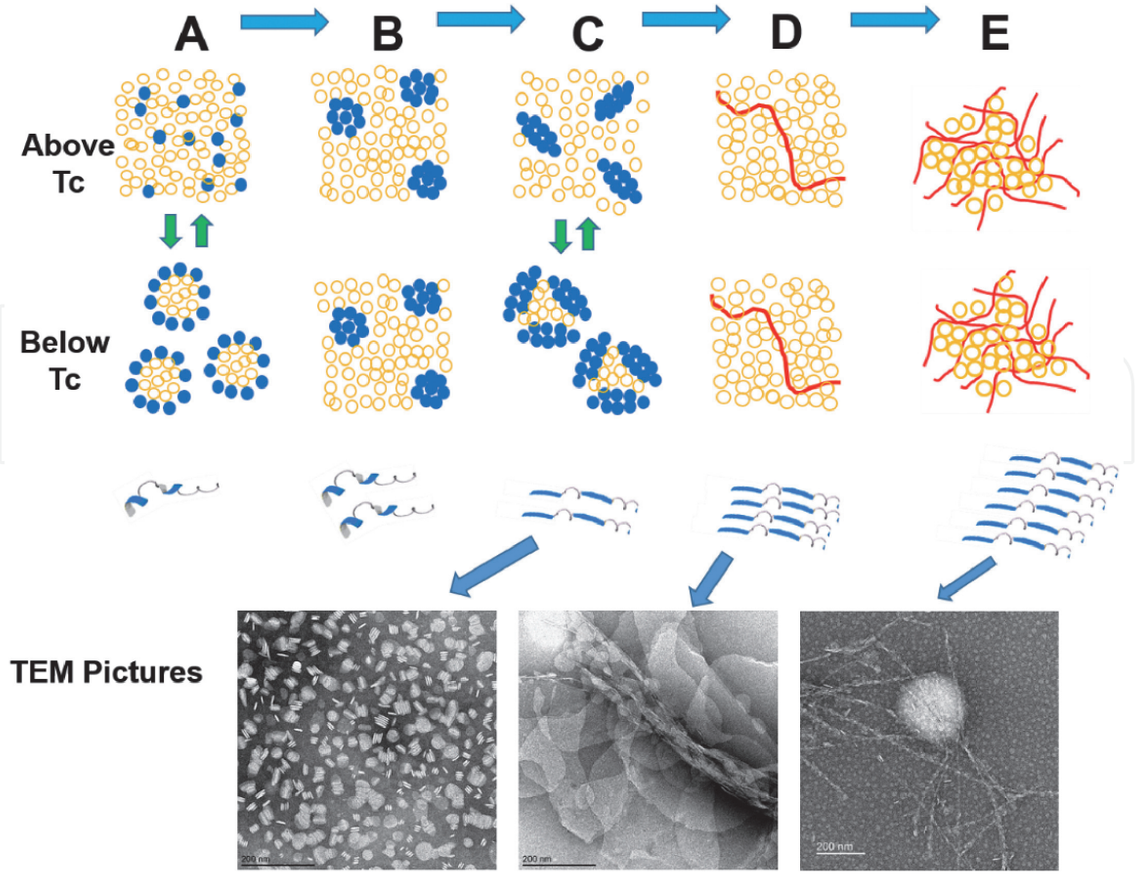

Figure 8.
Schematic diagrams of the morphological states of glucagon-DMPC bilayer systems (DMPC/glucagon; 50/1) at temperatures above and below the phase transition temperature (Tc = 23°C for DMPC). (A) Glucagon-DMPC bilayer state 1 day after sample preparation. (B) Glucagon-DMPC bilayer state 2 days after sample preparation. (C) Glucagon-DMPC bilayer state 4 days after sample preparation with the corresponding TEM picture shown below. (D) Glucagon-DMPC bilayer state 7 days after sample preparation with the corresponding TEM picture shown below. (E) Glucagon-DMPC bilayer system 10 days after sample preparation. The corresponding TEM picture is shown below (ref. [42]).

acidic solution. In an acidic solution, glucagon locates on the surface of lipid bilayer and then migrates laterally on the surface of the lipid bilayer to form oligomers and subsequently changes to fibril nuclei through homogeneous nucleation reaction. In contrast, glucagon is deeply embedded inside a lipid bilayer in neutral solution and thus migrates more slowly inside the lipid bilayer, as reflected in the lower k_1 value.

The k_2 rate constant for the elongation of glucagon fibrils in a DMPC/glucagon bilayer is much slower than that in neutral solution. Glucagon molecules in a DMPC/glucagon bilayer interact strongly with the DMPC bilayer. It therefore takes a long time to disrupt the interaction with the lipid bilayer and form interaction with glucagon fibrils. The k_2 rate constant for fibril elongation in the presence of lipid bilayers under neutral condition is significantly slower than that in lipid bilayers under acidic conditions. Under neutral conditions, glucagon is embedded deep inside the lipid bilayer, and hence it takes longer to release monomeric glucagon from the lipid bilayer. Therefore, the k_2 values for fibril elongation decrease as compared to the case in a lipid bilayer in acidic conditions.

7. Conclusions

It is demonstrated that glucagon forms fibrils in acidic solution and in the presence of lipid bilayer (bicelle) in acidic solution. Glucagon aggregates to form

fibril intermediates that glow into elongated fibrils. Glucagon intermediates are formed on the surface of the lipid bilayer in the presence of bicelle. These fibrils are cytotoxic through their activation of apoptotic processes, similar to β-amyloid and salmon calcitonin. Kinetic analyses of glucagon fibril formation are performed using a two-step autocatalytic reaction mechanism comprising fibril nucleation and elongation processes. It is revealed that glucagon forms fibril intermediates and grows into elongated fibrils inside the lipid bilayer under neutral conditions. These properties of glucagon fibril formation indicate that the interaction of the glucagon fibril with lipid bilayers is strongly dependent on the process of fibril formation. A neutral system is thus considered to reflect the fibril formation process in biological cells and provides insight into the mechanism underlying cytotoxicity of glucagon fibrils.

Acknowledgements

This work was supported by Grants-in-Aid for Scientific Research in an Innovative Area (JP16H00756 to AN) and by Grants-in-Aid for Scientific Research (C) (JP15K06963 to AN) from the Ministry of Culture, Sports, Science and Technology of Japan. The author wishes to thank Izuru Kawamura and Yoshiteru Makino for the discussion on this study and Izumi Yamane, Ayano Momose, Hideki Fujita, Eri Yoshimoto, Akie Kikuchi-Kinoshita, and Kazumi Haya for their experimental assistances.

Conflict of interest

The authors declare no conflict of interest.

Author details

Akira Naito
Graduate School of Engineering, Yokohama National University, Yokohama, Japan

*Address all correspondence to: naito@ynu.ac.jp

References

[1] Bromer WW, Sinn LG, Behrens OK. The amino acid sequence of glucagon. V. Location of amide groups, acid degradation studies and summary of sequential evidence. Journal of the American Chemical Society. 1957; **79**:2807-2810. DOI: 10.1021/ja01568a038

[2] Pohl SL, Birnbaumer L, Rodbell M. Glucagon-sensitive adenyl cyclase in plasma membrane of hepatic parenchymal cells. Science. 1969;**164**: 566-567. DOI: 10.1126/science.164.3870

[3] Rodbell M, Birnbaumer L, Pohl SL, Sundby F. The reaction of glucagon with its receptor: Evidence for discrete regions of activity and binding in the glucagon molecule. Proceedings of the National Academy of Sciences of the United States of America. 1971;**68**: 909-913. DOI: 10.1073/pnas.68.5.3870

[4] Beaven GH, Gratzer WB, Davies HG. Formation and structure of gels and fibrils from glucagon. European Journal of Biochemistry. 1969;**11**:37-42. DOI: 10.1111/j.1432.1033.1969.tb00735.x

[5] Onoue S, Ohshima K, Debari K, Koh K, Shioda S, Iwasa S, et al. Mishandling of the therapeutic peptide glucagon generates cytotoxic amyloidogenic fibrils. Pharmaceutical Research. 2004;**21**:1274-1283. DOI: 10.1023/B.PHAM.0000033016.36825.2c

[6] Kamgar-Parsi K, Tolchard J, Habenstein B, Loquet A, Naito A, Ramamoorthy A. Structural biology of calcitonin: From aqueous therapeutic properties to amyloid aggregation. Israel Journal of Chemistry. 2017;**57**:634-650. DOI: 10.1002/ijch.201600096

[7] Burke MJ, Rougvie MA. Cross-β protein structures. I. Insulin fibrils. Biochemistry. 1972;**11**:2435-2439. DOI: 10.1021/bi00763a008

[8] Prusiner SB. Prions. Proceedings of the National Academy of Sciences of the United States of America. 1998;**95**: 13363-13383. DOI: 10.1073/pnas.95.23.13363

[9] Cooper GJS, Willis AC, Clark A, Turner RC, Sim RB, Reid KBM. Purification and characterization of a peptide from amyloid-rich pancreases of type 2 diabetic patients. Proceedings of the National Academy of Sciences of the United States of America. 1987;**84**: 8628-8632. DOI: 10.1073/pnas.95.23.13363

[10] Vines G. Alzheimer's disease – From cause to cure? Trends in Biotechnology. 1993;**11**:49-55. DOI: 10.1016/0167-7799(93)90122-p

[11] Scherzinger E, Lurz R, Turmaine M, Mangiarini L, Hollenbach B, Hasenbank R, et al. Huntington-encoded polyglutamine expansions from amyloid-like protein aggregates in vitro and in vivo. Cell. 1997;**90**: 549-558. DOI: 10.1016/S0092-8674(00)80514-0

[12] Sipe JD. Amyloidosis. Annual Review of Biochemistry. 1992;**61**: 947-975. DOI: 10.1146/annurev.bi.61.070192.004503

[13] Sipe JD, Cohen AS. History of the amyloid fibril. Journal of Structural Biology. 2000;**130**:88-98. DOI: 10.1004/jsbi.2000.4221

[14] Kamihira M, Naito A, Tuzi S, Nosaka AY, Saitô H. Conformational transition and fibrillation mechanism of human calcitonin as studied by high-resolution solid-state ^{13}C NMR. Protein Science. 2000;**9**:867-877. DOI: 10.1110/ps.9.5.867

[15] Itoh-Watanabe H, Kamihira-Ishijima M, Javkhlantugs N, Inoue R,

Itoh Y, Endo H, et al. Role of aromatic residues in amyloid fibril formation of human calcitonin by solid-state ^{13}C NMR and molecular dynamics simulation. Physical Chemistry Chemical Physics. 2013;**15**:8890-8901. DOI: 10.1039/c3cp44544e

[16] Itoh-Watanabe H, Kamihira-Ishijima M, Kawamura I, Kondoh M, Nakakoshi M, Sato M, et al. Characterization of the spherical intermediates and fibril formation of hCT in HEPES solution using solid-state ^{13}C-NMR and transmission electron microscopy. Physical Chemistry Chemical Physics. 2013;**15**:16956-16964. DOI: 10.1039/c3cp52810c

[17] Kamgar-Parsi K, Hong L, Naito A, Brooks CL III, Ramamoorthy A. Growth-incompetent monomers of human calcitonin lead to a noncanonical direct relationship between peptide concentration and aggregation lag time. The Journal of Biological Chemistry. 2017;**292**:14963-14976. DOI: 10.1074/jbcM117.791236

[18] Gorman PM, Chakrabartty A. Alzheimer β-amyloid peptides: Structures of amyloid fibrils and alternate aggregation products. Peptide Science. 2001;**60**:381-394. DOI: 10.1002/1097-0282(2001)60:5<381::AID-BIP/0173>3.0.CO;2-U

[19] Tycko R. Insights into the amyloid folding problem from solid-state NMR. Biochemistry. 2003;**42**:3151-3159. DOI: 10.1021/bi027378p

[20] Tycko R. Application of solid state NMR to the structural characterization of amyloid fibrils: Methods and results. Progress in Nuclear Magnetic Resonance Spectroscopy. 2003;**42**:53-68. DOI: 10.1016/S0079-6565(03)00003-7

[21] Petkova AT, Yan W-M, Tycko R. Experimental constraints on quaternary structure in Alzheimer's β-amyloid fibrils. Biochemistry. 2006;**45**:498-512. DOI: 10.21/bi051952q

[22] Xiao Y, Ma B, McElheny D, Parthasarathy S, Long F, Hoshi M, et al. Aβ(1-42) fibril structure illuminates self-recognition and replication of amyloid in Alzheimer's disease. Nature Structural & Molecular Biology. 2015;**22**:499-505. DOI: 10.1038/nsmb.2991

[23] Wälti MA, Ravotti F, Arai H, Glabe CG, Wall JS, Böckmann A, et al. Atomic-resolution structure of a disease-relevant Aβ(1-42) amyloid fibril. Proceedings of the National Academy of Sciences of the United States of America. 2016;**113**:E4976-E4984. DOI: 10.1073/pnas1600749113

[24] Colvin MT, Silvers R, Ni QZ, Can TV, Sergeyev I, Rosay M, et al. Atomic resolution structure of monomorphic $A\beta_{42}$ amyloid fibrils. Journal of the American Chemical Society. 2016;**138**:9663-9674. DOI: 10.1021/jacs.6b05129

[25] Sasaki K, Dockerill S, Adamiak DA, Tickle IJ, Blundell T. X-ray analysis of glucagon and its relationship to receptor binding. Nature. 1975;**257**:751-757. DOI: 10.1038/257751a0

[26] Boesch C, Bundi A, Oppliger M, Wüthrich K. ^{1}H nuclear-magnetic-resonance studies of the molecular conformation of monomeric glucagon in aqueous solution. European Journal of Biochemistry. 1978;**91**:209-214. DOI: 10.111/j.1432-1033.1978.tb2095.x

[27] Braun W, Winder G, Lee KH, Wüthrich K. Conformation of glucagon in a lipid-water interphase by ^{1}H nuclear magnetic resonance. Journal of Molecular Biology. 1983;**169**:921-948. DOI: 10.1016/50022-2836(83)80143-0

[28] Onoue S, Iwasa S, Kojima T, Katoh F, Debari K, Koh K, et al.

Structural transition of glucagon in the concentrated solution observed by electrophoretic and spectroscopic techniques. Journal of Chromatography. A. 2006;**1109**:167-173. DOI: 10.1016/j.chroma.2005.11.130

[29] Pedersen JS, Dikov D, Flink JI, Hijuler HA, Christiansen G, Otzen DE. The changing face of glucagon fibrillation: Structural polymorphism and conformational imprinting. Journal of Molecular Biology. 2006;**355**:501-523. DOI: 10.1016/j.jmb.2006.09.100

[30] Pedersen JS, Andersen CB, Otzen DE. Amyloid structure–one but not the same: The many levels of fibrillar polymorphism. FEBS Journal. 2010;**277**:4591-4601. DOI: 10.1111/j.1742-4658.2010.07888.x

[31] Košmrlj A, Cordsen P, Kyrsting A, Otzen DE, Oddershede LB, Jensen MH. A monomer-trimer model supports intermittent glucagon fibril growth. Scientific Reports. 2015;**5**:9005. DOI: 10.1038/srep09005

[32] Naito A, Kawamura I. Solid-state NMR as a method to reveal structure and membrane-interactions of amyloidogenic protein and peptide. Biochimica et Biophysica Acta. 1768; **2007**:1900-1912. DOI: 10.1016/j.bbamem.2007.03.025

[33] Brender JR, Salamekh S, Ramamoorthy A. Membrane disruption and early events in the aggregation of the diabetes related peptide IAPP from a molecular perspective. Accounts of Chemical Research. 2012;**45**:454-462. DOI: 10.1021/ar200189b

[34] Kotler SA, Walsh P, Brender JR, Ramamoorthy A. Differences between amyloid-β aggregation in solution and on the membrane: Insights into elucidation of the mechanistic details of Alzheimer's disease. Chemical Society Reviews. 2014;**43**:6692-6700. DOI: 10.1039/c3cs60431d

[35] Matsuzaki K. How do membranes initiate Alzheimer's disease? Formation of toxic amyloid fibrils by the amyloid β-protein on ganglioside clusters. Accounts of Chemical Research. 2014; **47**:2397-2404. DOI: 10.1021/ar50012721

[36] Yamane I, Momose A, Fujita H, Yoshimoto E, Kikuchi-Kinoshita A, Kawamura I, et al. Fibrillation mechanism of glucagon in the presence of phospholipid bilayers as revealed by ^{13}C solid-state NMR spectroscopy. Chemistry and Physics of Lipids. 2019; **219**:36-44. DOI: 101016/j.chemphyslip.2019.01.008

[37] Epand RM, Jones AJS, Schreier S. Interaction of glucagon with dimyristoyl glycerophosphocholine. Biochimica et Biophysica Acta. 1977;**491**:296-304. DOI: 10.1016/0005-2795(77)90065-4

[38] Epand RM. Studies on the effect of the lipid phase transition on the interaction of glucagon with dimyristoyl glycerophosphocholine. Biochimica et Biophysica Acta. 1978;**514**:185-197. DOI: 10.1016/0005-2736(78)90290-0

[39] Epand RM, Epand RF, Stewart TP, Hu SW. The condensing effect of glucagon on phospholipid bilayers. Biochimica et Biophysica Acta. 1981; **649**:608-615. DOI: 10.1016/0005-2736(81)90165-6

[40] Naito A, Nagao T, Norisada K, Mizuno T, Tuzi S, Saitô H. Conformation and dynamics of melittin bound to magnetically oriented lipid bilayers by solid-state ^{31}P and ^{13}C NMR spectroscopy. Biophysical Journal. 2000;**78**:2405-2417. DOI: 10.1016/S0006-3495(00)76784-1

[41] Toraya S, Nagao T, Norisada K, Tuzi S, Saitô H, Izumi S. Morphological behavior of lipid bilayers induced by melittin near the phase transition temperature. Biophysical Journal. 2005; **89**:3214-3222. DOI: 10.1529/biophysj.105.059311

[42] Haya K, Makino Y, Kikuchi-Kinoshita A, Kawamura I, Naito A. ^{31}P and ^{13}C Solid-state NMR analysis of morphological changes of phospholipid bilayers containing glucagon during fibril formation of glucagon under neutral condition. Biochim. Biophys. Acta Biomembrane. Forthcoming issue. 2020. DOI: 10.1016/j.bbamem.2020.183290

[43] Andersen CB, Yagi H, Manno M, Martorana V, Ban T, Christiansen G, et al. Branching in amyloid fibril growth. Biophysical Journal. 2000;**96**:1529-1536. DOI: 10.1016/j.bpj.2008.11.024

[44] Andersen CB, Otzen D, Christiansen G, Rischel C. Glucagon amyloid-like fibril morphology is selected via morphology-dependent growth inhibition. Biochemistry. 2007; **46**:7314-7324. DOI: 10.1021.bi6025374

[45] Andersen CB, Hicks MR, Vetri V, Vandahl B, Rahbek-Nielsen H, Thogersen H, et al. Glucagon fibril polymorphism reflects differences in protofilament backbone structure. Journal of Molecular Biology. 2010;**397**: 932-946. DOI: 10.1016/j.jmb.2010.02.012

[46] Jong KLD, Incledon B, Yip CM, DeFelippis MR. Amyloid fibrils of glucagon characterized by high-resolution atomic force microscopy. Biophysical Journal. 2006;**91**:1905-1914. DOI: 10.1529/biophysj.105.077438

[47] Saitô H. Conformation-dependent ^{13}C chemical shifts: A new means of conformation characterization as obtained by high-resolution solid-state ^{13}C NMR. Magnetic Resonance in Chemistry. 1986;**24**:835-852. DOI: 10.1002/mrc.1260241.002

[48] Saitô H, Ando I. High-resolution solid-state NMR studies of synthetic and biological macromolecules. Annual Reports on NMR Spectroscopy. 1989;**21**: 209-290. DOI: 10.1016/50066-4103(08)60124-6

[49] Saitô H, Ando I, Ramamoorthy A. Chemical shift tensor – The heart of NMR: Insight into biological aspect proteins. Progress in Nuclear Magnetic Resonance Spectroscopy. 2010;**57**: 181-228. DOI: 10.1016/j.pnmrs.2010.04.005

[50] Onoue S, Ohshima K, Endo K, Yajima T, Kashimoto K. PACAP protects neuronal PC12 cells from the cytotoxicity of human prion protein fragment 106-125. FEBS Letters. 2002; **522**:65-72. DOI: 10.1016/50014-5793(02)02886-7

[51] Onoue S, Endo K, Ohshima K, Yajima T, Kashimoto K. The neuropeptide PACAP attenuates b-amyloid (1-42)-induced toxicity in PC12 cells. Peptides. 2002;**23**:1471-1478. DOI: 10.1016/S0196-9781(02)00085-2

[52] Kamihira-Ishijima M, Nakazawa H, Kira A, Naito A, Nakayama T. Inhibitory mechanism of pancreatic amyloid fibril formation: Formation of the complex between tea catechins and the fragment of residue 22-27. Biochemistry. 2012;**51**:10167-10174. DOI: 10.101021/bi3012274

[53] Azakami H, Mukai A, Kato A. Role of amyloid cross β-structure in the formation of soluble aggregate and gel in heat-induced ovalbumin. Journal of Agricultural and Food Chemistry. 2005; **53**:1254-1257. DOI: 10.1021/jf049325f

[54] Corrigan AM, Donald AM. Particle tracking microrheology of gel-forming amyloid fibril networks. European Physical Journal E: Soft Matter and Biological Physics. 2009;**28**:457-462. DOI: 10.1140/epje/12008-10439-7